AD_____

**AWARD NUMBER: W81XWH-15-1-0341**

**TITLE:** High Spatiotemporal Resolution Prostate MRI

**PRINCIPAL INVESTIGATOR:** Stephen J. Riederer

**CONTRACTING ORGANIZATION:**

**REPORT DATE: September 2016**

**TYPE OF REPORT:** Annual

**PREPARED FOR:** U.S. Army Medical Research and Materiel Command
Fort Detrick, Maryland 21702-5012

# REPORT DOCUMENTATION PAGE

*Form Approved*
*OMB No. 0704-0188*



| 1. REPORT DATE | 2. REPORT TYPE | 3. DATES COVERED |
|---|---|---|
| September 2016 | Annual | 15 Aug 2015 - 14 Aug 2016 |

**4. TITLE AND SUBTITLE**

High Spatiotemporal Resolution Prostate MRI

**5a. CONTRACT NUMBER**

**5b. GRANT NUMBER**
W81XWH-15-1-0341

**5c. PROGRAM ELEMENT NUMBER**

**6. AUTHOR(S)**

Stephen J. Riederer

E-Mail: Riederer@mayo.edu

**5d. PROJECT NUMBER**

**5e. TASK NUMBER**

**5f. WORK UNIT NUMBER**

**7. PERFORMING ORGANIZATION NAME(S) AND ADDRESS(ES)**

Mayo Clinic
200 1st ST SW
Rochester, MN 55905-0002

**8. PERFORMING ORGANIZATION REPORT NUMBER**

**9. SPONSORING / MONITORING AGENCY NAME(S) AND ADDRESS(ES)**

U.S. Army Medical Research and Materiel Command
Fort Detrick, Maryland 21702-5012

**10. SPONSOR/MONITOR'S ACRONYM(S)**

**11. SPONSOR/MONITOR'S REPORT NUMBER(S)**

**12. DISTRIBUTION / AVAILABILITY STATEMENT**

Approved for Public Release; Distribution Unlimited

**13. SUPPLEMENTARY NOTES**

**14. ABSTRACT**

Prostate cancer (PCa) is the second leading cause of cancer death in men. However, when detected and treated promptly the five-year relative survival rate approaches 100%. The overall purpose of this project is to develop improved means using MRI for detecting prostate cancer with the potential for differentiating disease aggressiveness. The hypothesis is that dynamic whole-volume contrast-enhanced perfusion imaging of the prostate gland can be performed with 1 mm isotropic spatial resolution and 2 sec frame times, providing an order of magnitude improvement over current techniques. The specific aims are: (i) to develop an MRI acquisition technique for time-resolved 3D MRI of the prostate, (ii) to develop a fundamentally new coil element family having variable sensitivity along the superior-to-inferior direction, (iii) to incorporate partial Fourier and acceleration methods into high speed reconstruction to provide high quality 3D images in real time at frame times of 2 sec or less.

**15. SUBJECT TERMS**

Prostate Cancer, Dynamic-Contrast-Enhanced Prostate MRI

| 16. SECURITY CLASSIFICATION OF: | | | 17. LIMITATION OF ABSTRACT | 18. NUMBER OF PAGES | 19a. NAME OF RESPONSIBLE PERSON |
|---|---|---|---|---|---|
| a. REPORT | b. ABSTRACT | c. THIS PAGE | | | USAMRMC |
| Unclassified | Unclassified | Unclassified | Unclassified | 39 | 19b. TELEPHONE NUMBER *(include area code)* |

## TABLE OF CONTENTS

## 1. INTRODUCTION

Prostate cancer (PCa) is the second leading cause of cancer death in men after lung cancer. Approximately one in nine men will be diagnosed with prostate cancer but when detected early and treated promptly the five-year relative survival rate approaches 100%. The motivation of this project is to develop improved means for detecting prostate cancer. Magnetic resonance imaging (MRI) has been applied to the imaging of prostate cancer for several decades. The typical MRI prostate exam today consists of several "pulse sequences:" (i) T2-weighted spin-echo imaging; (ii) diffusion-weighted imaging (DWI); (iii) dynamic contrast-enhanced (DCE) perfusion MRI. While prostate cancer can be visualized using each sequence, only sequence (iii) provides dynamic information about the temporal enhancement pattern of any PCa lesions. The purpose of this project is to develop 10× improved spatiotemporal resolution DCE-MRI of prostate.

## 2. KEYWORDS

| | |
|---|---|
| CAPR | Cartesian Acquisition with Projection Reconstruction-like sampling |
| CE-MRA | Contrast-Enhanced Magnetic Resonance Angiography |
| DCE-MRI | Dynamic-Constrast-Enhanced Magnetic Resonance Imaging |
| MRI | Magnetic Resonance Imaging |
| PCa | Prostate Cancer |
| R | Acceleration Factor |
| SENSE | Sensitivity Encoding (a type of MRI acceleration technique) |
| SNR | Signal-to-Noise Ratio |

## 3. ACCOMPLISHMENTS:

**What were the major goals of the project?**

Tasks for Months 1-12 (encompassing August 15, 2015 through August 14, 2016) taken from the grant application Statement of Work are shown below. All tasks have been completed, with the completion month shown in **red (in parentheses)**.

| **Specific Aim 1: Development of MRI Acquisition Method** | **Months** | **Investigator** |
|---|---|---|
| Major Task 1: Optimization of pCAPR Pulse Sequence Applied to Prostate Imaging | | |
| Subtask 1.1: Determine parameter options for various spatiotemporal resolution combinations | 1-6 **(5)** | Dr. Riederer; Dr. Kawashima; Mr. Borisch |
| Subtask 1.2: Design, construct, and test phantom which mimics geometry for prostate MRI | 1-6 **(6)** | Dr. Riederer; Mr. Hulshizer |
| Subtask 1.3: Experimentally test and evaluate versions of pulse sequence with prostate phantom and select optimum sequence with standard receiver coil array | 6-12 **(9,ongoing)** | Dr. Riederer; Mr. Hulshizer |
| **Specific Aim 2: Development of Special Purpose Receiver Coil Arrays** | | |

| | | |
|---|---|---|
| Major Task 2: Optimization of pCAPR Pulse Sequence Applied to Prostate Imaging | | |
| Subtask 2.1: Select optimum triangular element size and construct matched single pair of coils | 1-6 **(3)** | Dr. Riederer; Mr. Hulshizer |
| Subtask 2.2: Construct, tune, and match multiple pairs of triangular coils | 7-12 **(9)** | Dr. Riederer; Mr. Hulshizer |
| **Specific Aim 3: Formation of Optimized pCAPR Images** | | |
| Major Task 3.1: Image Reconstruction and System Integration | | |
| Subtask 3.1: Allowance for arbitrary acceleration factors ($R_Y$,$R_Z$) and CAIPIRINHA kernels for arbitrary R | 1-6 **(6)** | Mr. Borisch |
| Subtask 3.2: Incorporate pCAPR pulse sequence into image reconstruction framework | 7-12 **(7)** | Mr. Borisch |

**What was accomplished under these goals?**

The Statement of Work is divided into three specific aims with subtasks for each. Progress has been made for each aim. The following paragraphs are associated with specific subtasks identified in the Statement of Work (SOW).

Specific Aim 1

*Subtask 1.1.*

For this subtask parameter sets for various combinations of spatial and temporal resolution and acceleration factor (R) were evaluated using g-factor analysis, signal-to-noise ratio (SNR), and radiologist preference. Two target applications of dynamic-contrast-enhanced (DCE) MRI with potentially different spatiotemporal resolution were defined by our collaborating radiologist. The first application is used to image patients suspected of prostate cancer. In this case "high" temporal resolution of 6-8 sec per image is desired. The second application is for patients who have undergone intervention such as prostatectomy or radiation therapy for prostate cancer but have had subsequent nonzero PSA measurements. For these cases of what is referred to as "biochemical recurrence" high spatial resolution is desired with potentially coarser image update times. G-factor analysis takes images of the sensitivity across the 3D volume of each individual coil element and

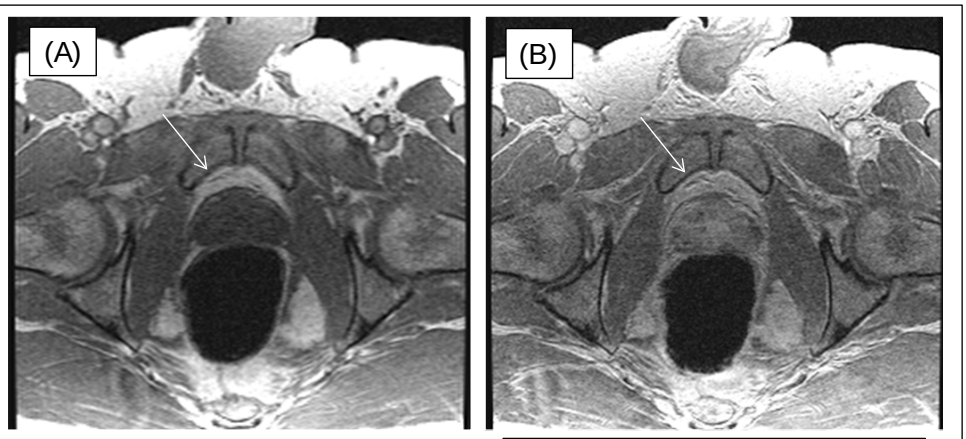


Figure 1. Axial images of prostate in the same subject. Example of standard (A) and high (B) spatial resolution images. Arrow points to edge of pubic symphysis as an example of improved sharpness in (B). (A) was taken from an image sequence with higher (6.5 sec) temporal resolution than (B) (15.0 sec).

algebraically computes the level of noise amplification when acceleration is performed. As increased acceleration factors R are used in the acquisition, the resultant SNR deteriorates. Folding these considerations of adequate SNR and target spatiotemporal resolution together, two target working parameter sets have been identified and implemented in baseline acquisitions. The parameter sets are indicated and resultant images illustrated in Figure 1 for the pre-intervention prostate patient (A) and for the biochemical recurrence application (B). The arrows identify one specific anatomic feature which illustrates the improved spatial resolution in (B).

*Subtask 1.2.*

For Subtask 1.2 we have designed and constructed a phantom which mimics the male pelvis for MR imaging (Figure 2). We started with a plastic shell of the male pelvis which corresponds to a male with BMI of approximately 25.. We wished to incorporate inclusions to simulate both the bladder and the prostate gland. This was done using latex balloons filled with 50 ml of differing B-gel solutions as shown in (A). These balloons were then positioned within the overall plastic shell while it was filled with B-gel, sorbic acid, and NaCl in distilled water. The solution then solidifies. A photograph of the final phantom is shown in (B), with marking showing the locations of the two inclusions. The overall weight is 21.5 kg. We have initiated studies for Subtask 1.3 in which MR images are acquired (e.g. C). Such images were used to aid in selecting the optimum sequence parameters Aim #1.

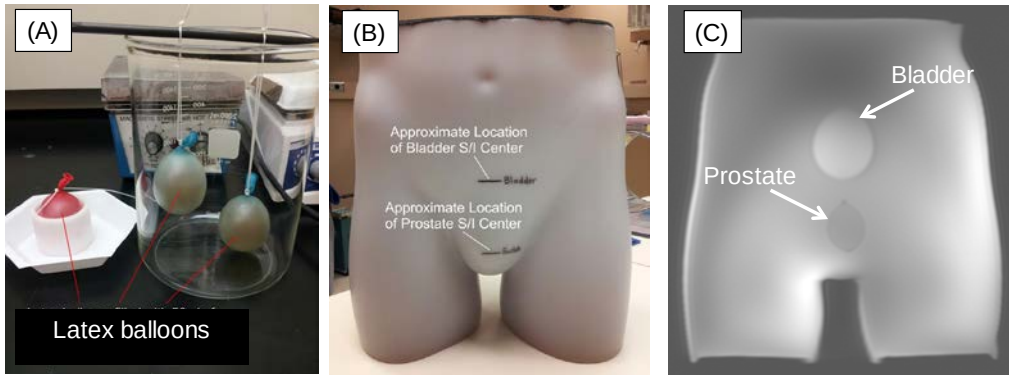


Figure 2. Male pelvis phantom. Figure parts are described in text.

Specific Aim 2

*Subtask 2.1.*

For Subtask 2.1 we evaluated a variety of triangular coil elements with different apex angles and sizes using simulations based on the Biot-Savart Law as well as experimental measurements of sensitivity. Sample results of a simulation are shown in Figure 3A. This shows the sensitivity across a plane at a depth of 10 cm from an assumed triangular element with each element shown as the white outline. As desired, the sensitivity varies along the x-direction of the plot (left-right for these), corresponding to the superior-inferior (S/I)

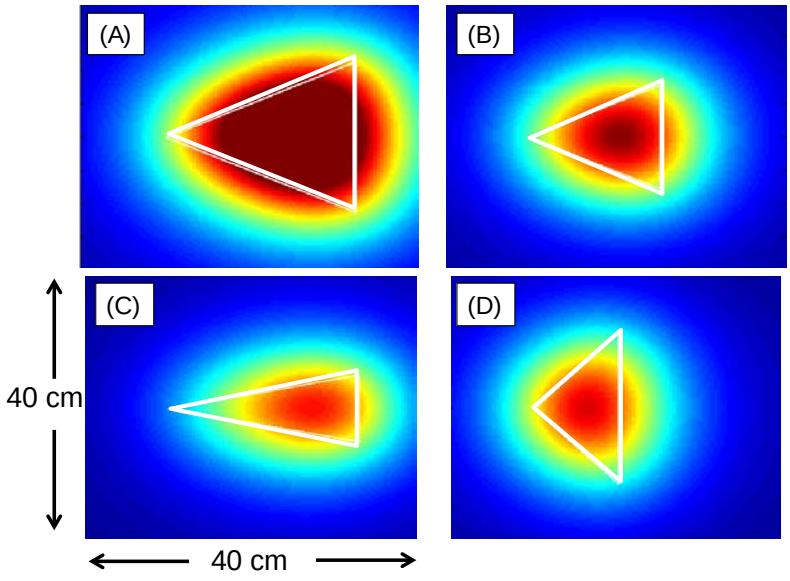


Figure 3. Plots of sensitivity of triangular-shaped coils at a fixed depth 10 cm from the coil face. Coil element outline is shown in white for each with same color scale for all cases. Triangle Base × Height values are (cm) (A) 22.5 × 22.5; (B) 15.5 × 15.5; (C) 22.5 × 10.0; (D) 10.0 × 22.5.

direction for a patient. From results like this the coil element in (A) was large enough to have adequate sensitivity at depth and had adequate variation of sensitivity along the x-direction. This element (22.5 cm base × 22.5 cm height) was chosen for further study. Use of the sensitivity data from a single coil was then replicated at assumed coil locations and then used together to synthesize multi-coil acquisition. From this information g-factor maps were calculated. Based on results to minimize g-factor for acceleration factors no higher than about R = 4 as well as consideration of the need to image a S/I field of view of 10 cm or more to encompass the prostate, this coil element size was chosen for construction.

*Subtask 2.2.*

For Subtask 2.2 two pairs of elements, four elements total, of this target size were constructed. Use of such paired modules allows patient-specific selection of the number of modules as based on patient size. Two such modules are shown in Figure 4. This will be further studied during the next funding period. Part of this study will be to compare performance of the proposed triangular-element-based array with other multi-element arrays.

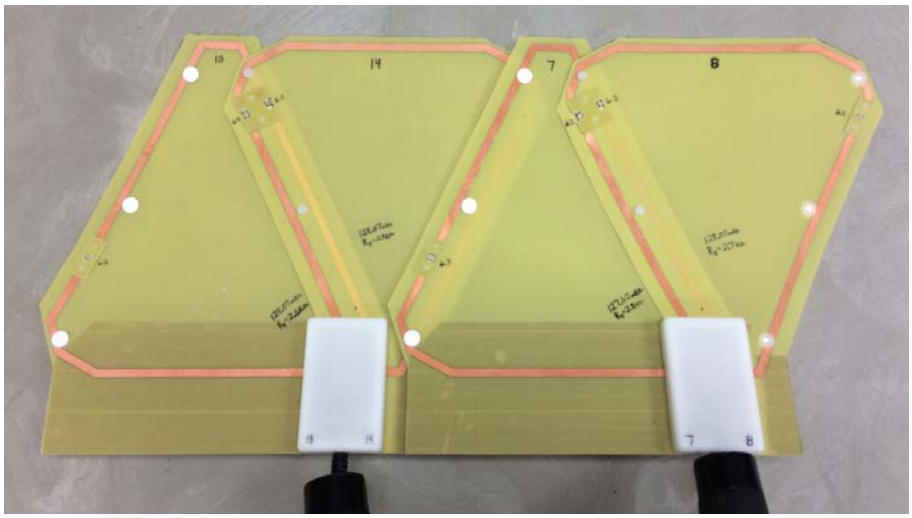

Figure 4. Photograph of two two-element modules based on the triangular element design. Each element is 22.5 cm base × 22.5 cm height.

Specific Aim 3

*Subtask 3.1.*

For Subtask 3.1 we have modified our reconstruction software to allow for arbitrary acceleration factors and kernels as desired. Examples of this were shown previously in Figure 1 in which the image in (A) was reconstructed using SENSE acceleration $R = R_Y \times R_Z = 2.50 \times 1.12 = 2.80$ while that in (B) used $R = 3.56 \times 1.27 = 4.17$.

*Subtask 3.2.*

For Subtask 3.2 we have installed the basic dynamic contrast-enhanced (DCE-MRI) pulse sequence based on our CAPR k-space sampling onto several GE 3.0 Tesla MRI scanners and developed the software to direct the acquired MRI data to our custom computation hardware for online reconstruction as shown schematically in Figure 5. This allows rapid

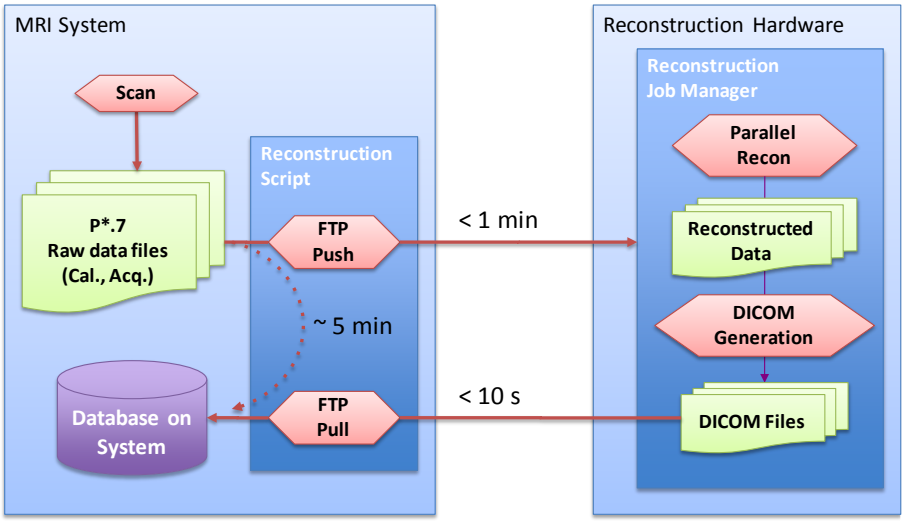


Figure 5. Schematic showing host MRI scanner (left) and custom computation hardware (right).

reconstruction of scans made of phantoms or of human subjects originating from multiple MRI scanners across Mayo.

We are pleased with the progress made during the first funding cycle of this grant.

**What opportunities for training and professional development has the project provided?**
Nothing to report.

**How were the results disseminated to communities of interest?**
Nothing to report other than that in Section 6 of this report.

**What do you plan to do during the next reporting period to accomplish the goals?**
We will continue our work according to the tasks shown in the original Statement of Work.

4. **IMPACT:** Describe distinctive contributions, major accomplishments, innovations, successes, or any change in practice or behavior that has come about as a result of the project relative to:

**What was the impact on the development of the principal discipline(s) of the project?**
The tasks completed in the first nine months of this three-year project provide a good basis for ongoing work for all three Aims in the months ahead.

**What was the impact on other disciplines?**
Nothing to Report. We note, however, that improvements in coils and acceleration techniques for prostate DCE-MRI, the specific area of study of this grant, may prove to have benefits for other MRI methods for prostate imaging as well as for MRI of the pelvis in general.

**What was the impact on technology transfer?**
Our baseline DCE-MRI pulse sequences are now used clinically at Mayo Clinic. Our clinical practice at Mayo Rochester currently performs five to ten such exams per day.

**What was the impact on society beyond science and technology?**
Nothing to Report

5. **CHANGES/PROBLEMS:** The PD/PI is reminded that the recipient organization is required to obtain prior written approval from the awarding agency grants official whenever there are significant changes in the project or its direction. If not previously reported in writing, provide the following additional information or state, "Nothing to Report," if applicable:

**Changes in approach and reasons for change**
Nothing to Report

**Actual or anticipated problems or delays and actions or plans to resolve them**
Nothing to Report

**Changes that had a significant impact on expenditures**
Nothing to Report

**Significant changes in use or care of human subjects, vertebrate animals, biohazards, and/or select agents**

**Significant changes in use or care of human subjects**
Nothing to Report

**Significant changes in use or care of vertebrate animals**
Nothing to Report

**Significant changes in use of biohazards and/or select agents**
Nothing to Report

**6. PRODUCTS:** List any products resulting from the project during the reporting period. If there is nothing to report under a particular item, state "Nothing to Report."

- **Publications, conference papers, and presentations**
  Report only the major publication(s) resulting from the work under this award.

**Journal publications.**

1. Riederer SJ, Borisch EA, Froemming AT, Grimm RC, Kawashima A, Mynderse LA, Trzasko JD, "Improved performance of prostate DCE-MRI using a 32-coil vs. 12-coil receiver array." (in preparation)

**Books or other non-periodical, one-time publications.**
Nothing to Report

**Other publications, conference papers and presentations**.

1. Kargar S, Stinson EG, Borisch EA, Froemming AT, Kawashima A, Mynderse LA, Trzasko JD, Riederer SJ, "Robust and efficient estimation of optimum perfusion parameters in dynamic contrast-enhanced MRI of the prostate." 27th Annual Intl Conf on Magnetic Resonance Angiography, Cincinnati OH, Sept16-18, 2015.
2. Riederer SJ, Borisch EA, Froemming AT, Grimm RC, Kawashima A, Trzasko JD, "Improved SNR performance of prostate DCE-MRI using 32 receiver channels." Radiol Soc North America, Chicago IL, Nov 2015. PH251-SD-TUB5.
3. Kargar S, Stinson EG, Borisch EA, Froemming AT, Kawashima A, Mynderse LA, Trzasko JD, Riederer SJ, "An efficient variable projection strategy for pharmacokinetic parameter estimation inf prostate DCE-MRI." ISMRM Workshop on Data Sampling, Sedona AZ, January 10-14, 2016.
4. Riederer SJ, Borisch EA, Froemming AT, Grimm RC, Kawashima A, Trzasko JD, "Prostate DCE-MRI: improved SNR with 32-element receiver arrays." Annual Mtg Europ Cong Radiol, Vienna Austria, March 2-6, 2016.
5. Trzasko JD, Borisch EA, Froemming AT, Kawashima A, Warndahl BA, Grimm RC, Mynderse LA, Young PM, King BF, Stinson EG, Manduca A, Riederer SJ, "Sparse reconstruction of 4D prostate DCE-MRI: integration into routine clinical practice." Int'l Symp on Biomedical Imaging, Prague, Czech Republic, April 13-16, 2016.

- **Website(s) or other Internet site(s)**

Nothing to Report

- **Technologies or techniques**

Nothing to Report

- **Inventions, patent applications, and/or licenses**

Nothing to Report

- **Other Products**

Nothing to Report

## 7. PARTICIPANTS & OTHER COLLABORATING ORGANIZATIONS

**What individuals have worked on the project?**

| | |
|---|---|
| Name: | Stephen J. Riederer, Ph.D. |
| Project Role: | Principal Investigator |
| Nearest person month worked: | 1.8 |
| Contribution to Project: | Dr. Riederer directs all technical aspects of the projects. |
| Funding Support: | This DOD CDMRP grant |

| | |
|---|---|
| Name: | Akira Kawashima, M.D., Ph.D. |
| Project Role: | Co-Investigator |
| Nearest person month worked: | .22 |
| Contribution to Project: | Dr. Kawashima oversees feasibility testing performed in volunteers and provides feedback on intermediate results for all projects. |
| Funding Support: | This DOD CDMRP grant |

| | |
|---|---|
| Name: | Eric A. Borisch |
| Project Role: | Information Services Technical Specialist |
| Nearest person month worked: | 2.76 |
| Contribution to Project: | Mr. Borisch is responsible for writing and developing production-level software for all projects, software heavily centered on reconstruction of 2D-accelerated 3D data sets acquired with various view orders. |
| Funding Support: | This DOD CDMRP grant |

| | |
|---|---|
| Name: | Thomas C. Hulshizer |
| Project Role: | MR Technician |
| Nearest person month worked: | 1.2 |
| Contribution to Project: | Mr. Hulshizer is responsible for construction of the pelvis-prostate phantom, construction and tuning of RF coils, and testing of prototype MR pulse sequences using phantoms. |
| Funding Support: | This DOD CDMRP grant |

| | |
|---|---|
| Name: | Paul T. Weavers, Ph.D. |
| Project Role: | Graduate Student |
| Nearest person month worked: | .22 |
| Contribution to Project: | Dr. Weavers performed simulations and early testing of the triangle-shaped coils. |
| Funding Support: | Mayo Graduate School |

**Has there been a change in the active other support of the PD/PI(s) or senior/key personnel since the last reporting period?**

Stephen J. Riederer, Ph.D.
Ended December 2015:
Mayo Center for Individualized Medicine Imaging Biomarkers Program
"Functional Biomarkers of Prostate Cancer" (PI: SJ Riederer, Ph.D.)
Purpose: develop image processing methods for estimating prostate perfusion parameters
3.0 months/year (25% effort)

Started February 2016:
Mayo Discovery-Translation Program
"Advanced MRI Techniques for Prostate Cancer Imaging" (PI: JD Trzasko, Ph.D.)
Purpose: develop compressed sensing methods for estimating MRI-measured tissue parameters
0.36 months/year (3% effort)

Overlap: Although in the same general area of prostate MRI, there is no overlap of either of these above projects with the DOD grant. The DOD grant focuses on MR image acquisition of the prostate. These above grants both consider how MRI images can subsequently be analyzed to estimate various tissue parameters of normal and malignant prostate tissues.

**What other organizations were involved as partners?**

Nothing to Report other than the general support provided by the PI's institution, Mayo Clinic.

## 8. SPECIAL REPORTING REQUIREMENTS

None

## 9. APPENDICES:

Attach all appendices that contain information that supplements, clarifies or supports the text. Examples include original copies of journal articles, reprints of manuscripts and abstracts, a curriculum vitae, patent applications, study questionnaires, and surveys, etc.

**Manuscripts**

Attached is a copy of the manuscript being submitted for review:
"Improved Performance of Prostate DCE-MRI Using a 32-Coil vs. 12-Coil Receiver Array"

# Improved Performance of Prostate DCE-MRI Using a 32-Coil vs. 12-Coil Receiver Array

Stephen J. Riederer, Ph.D.

Eric A. Borisch

Adam T. Froemming, M.D.

Roger C. Grimm

Akira Kawashima, M.D., Ph.D.

Lance Mynderse, M.D.

Joshua D. Trzasko, Ph.D.

Mayo Clinic

200 First Street SW

Rochester, MN 55905

TITLE:

Improved Performance of Prostate DCE-MRI Using a 32-Coil vs. 12-Coil Receiver Array

ABSTRACT

Purpose: To assess whether acquisition with 32 receiver coils rather than the vendor-recommended 12 coils provides significantly improved performance in 3D dynamic contrast-enhanced MRI (DCE-MRI) of the prostate.

Materials: The study was approved by the institutional review board and was compliant with HIPAA. 50 consecutive male patients in whom prostate MRI was clinically indicated were prospectively imaged in March 2015 with an accelerated DCE-MRI sequence in which image reconstruction was performed using 12 and 32 coil elements. The two reconstructions were compared quantitatively and qualitatively. The first was done using signal-to-noise ratio (SNR) and g-factor analysis to assess sensitivity to acceleration. The second was done using a five-point scale by two experienced radiologists using criteria of perceived SNR, artifact, spatial resolution, and overall preference. Significance was assessed with the Wilcoxon signed rank test.

Results: Reconstruction using 32 coils provided improved performance based on SNR and g-factor statistics. For the qualitative assessment, reconstruction using 32 coils was rated significantly improved ($p<.001$) vs. 12 coils on the basis of perceived SNR and radiologist preference and equivalent for spatial resolution and artifact.

Conclusions: Reconstruction of 3D accelerated DCE-MRI studies of the prostate using 32 independent receiver coils provides improved overall performance vs. using 12 coils.

Keywords: prostate MRI, DCE-MRI, multi-element receiver coil

INTRODUCTION

MR imaging of the prostate is commonly performed using a multi-parametric approach in which multiple sequences are used to aid in radiologic interpretation (1-3). A commonly used pulse sequence within this exam is three-dimensional (3D) dynamic contrast-enhanced MRI (DCE-MRI) (4-6) in which a contrast agent is administered intravenously, and images are acquired of the prostate to observe washin and washout of the contrast-enhanced blood over the entire prostate volume. Because the desired spatiotemporal resolution of such a sequence typically pushes the limits of signal-to-noise ratio (SNR), the need for good performance of the receiver coils is important.

In approximately the last decade MRI vendors have enhanced their product offerings in several ways which can potentially benefit imaging of the abdomen and pelvis, including prostate MRI. These include receiver coil arrays contained within the patient table, larger diameter bore scanners to accommodate patients with large body habitus, and high-count receiver channels. As these systems have been installed there can be questions as to effective use.

Prostate MRI at our institution is principally performed using an MRI system with features similar to those described above. The vendor-recommended coil selection for prostate DCE-MRI calls for 12 channels of data acquisition to be used. This includes eight active elements from the array contained within the table posterior to the supine patient and four active elements used from a 16-element array placed anteriorly. In investigating to what extent the DCE-MRI sequence could be accelerated, we considered whether additional coil elements could

be used. To fully exploit the capability of the MRI system, the option for use of 32 channels was considered. Thus, the specific hypothesis of this work was that the use of 32 vs. 12 independent receiver coils would provide improved performance in DCE-MRI of the prostate. Similar studies of the potential advantage of an increased number of coil elements for a given pulse sequence have been performed for brain MRI (7-9).

## MATERIALS AND METHODS

This study was approved by the institutional review board which waived the need for written consent. The study was compliant with HIPAA.

### *Subjects*

50 consecutive male subjects for whom a prostate MRI exam was clinically indicated and who gave their assent for their exam results to be used for research purposes were prospectively enrolled in the study over the period March 10-27, 2015. The age, weight, and body mass index (BMI) ranges were 51 to 86 years, 63.5 to 155.1 kg, and 22.5 to 46.8, respectively. Forty-five of the 50 had intact prostates; 5 were evaluated post-prostatectomy.

### *MRI Acquisition*

All studies were performed on either of two identical 3.0 T MRI scanners (Discovery MR750w, GE Healthcare, Waukesha WI) utilizing an institutional clinical exam protocol. Each machine has a 70 cm diameter bore, a vendor-provided 40-element receiver coil array (Geometry Embracing Method “GEM” array) embedded within the patient table, and 32 receiver channels. Each patient exam included a localizer, T2-weighted spin-echo, and diffusion-weighted

sequences, followed by a DCE-MRI study performed with intravenous contrast administration. Details of the RF-spoiled gradient echo DCE-MRI sequence are shown in Table 1. Contrast material (Dotarem, Guerbet, Paris, France) was administered into an arm vein at a rate of 3 ml/sec followed by a 20 ml saline flush at 3 ml/sec. The contrast dose was 0.1 mmol/kg, with a maximum of 20 ml for patients weighing 100 kg or more.

The impetus for this study was to push the acceleration of the DCE-MRI sequence for improved spatiotemporal resolution. The sequence used is based on one developed for time-resolved contrast-enhanced MR angiography (CE-MRA) using two-dimensional (2D) SENSE acceleration (10). For this work the slab orientation was approximately axial but with slight forward tilting to align the slab select direction with the central axis of the prostate gland as determined in the sagittal localizer. SENSE acceleration factors of 2.49 and 1.12 were applied along the left/right (L/R) phase encode and approximate superior/inferior (S/I) slice encode directions, respectively, yielding a net acceleration factor of R = 2.78. DCE-MRI acquisition was initiated 20 sec prior to the start of contrast injection, the frame time was approximately 6.6 sec, and a total of 33 time frames were collected.

*Selection of Receiver Coil Elements*

This work made use of the 40-element GEM receiver coil array shown schematically in Figure 1A. The array consists of five columns of elements oriented longitudinally which for the supine patient are located posteriorly. Also used was a 16-element coil array placed anteriorly consisting of four longitudinally oriented columns each comprised of four elements (Fig. 1B).

The combinations of coil elements available for usage are limited by the vendor, and recommendations are made according to the type of exam. For prostate MRI this calls for 12 active receiver coil elements, eight from the GEM array and four from the anterior array. These are highlighted in yellow in Figs. 1A and B, respectively. The elements selected from the GEM array (A) are the two central-most elements which encompass the S/I extent of the prostate, as identified from the sagittal scout images, and the three elements from the next closest columns on each side. For the anterior coil (B) the two central elements from the two rows which similarly encompass the S/I extent of the prostate are selected. All other coil elements from both arrays are electronically disabled during acquisition, and data from the 12 elements are individually digitized and used in reconstruction.

To attempt to exploit the full 32-channel capability of the MRI systems for accelerated DCE-MRI, we next considered use of the vendor-allowed 16 elements from each array. This is also depicted in Figs. 1A-B. Coil elements used for the 12-element case were expanded to include those shown in blue. For the GEM coil (A) the two central-most elements best aligned with the S/I prostate extent are selected as before. The lateral rows containing those elements are supplemented with the rows of elements next positioned superiorly and inferiorly. For each row the leftmost and rightmost elements (e.g. elements 3 and 33 of Fig. 1A) are automatically combined in vendor hardware prior to digitization, in effect forming one virtual coil from two coil elements. Thus, the 20 elements contained within the four selected rows of the GEM coil are encoded in 16 individual coils, with four of these being two-element combinations. For the anterior array all 16 elements are used (B). It is noted that the channels used for the 12-coil acquisition are a subset of those used for the 32-coil reconstruction. The remaining 20 coil

elements located at the ends of the GEM array are electronically disabled during the 32-coil acquisition.

*Image Reconstruction*

Reconstruction was performed offline with standard SENSE unfolding (11) using a custom-built computing system described in (12). To avoid the complications and potential variability of performing two separate DCE-MRI studies on each subject, we investigated if a single 32-coil acquisition could be done and the 12-coil acquisition accurately simulated by using only the appropriate 12 data sets for reconstruction. The risk with this approach is that the electronically active but unused 20 coil elements in the 32-active-element acquisition would interfere through undesirable coupling with the 12 elements selected for reconstruction. To assess this we first performed test scans in a volunteer in which separate acquisitions were done with the 12-active-coil and 32-active-coil approaches using the accelerated DCE-MRI sequence without contrast injection. Unaccelerated coil calibration image sets were also acquired with both approaches. Data from the 32-coil acquisition were reconstructed two ways: (i) using all 32 coils; and (ii) using data from only the same 12 coils as for the 12-active-coil acquisition. Reconstruction (iii) was done using all 12 coils of the 12-active-coil acquisition.

The images from reconstructions (i), (ii), and (iii) were compared in two ways. First, images of absolute SNR were formed from data sets (i), (ii), and (iii) using the method of Refs. (13, 14). As the coil sensitivity profiles used in these calculations were estimated empirically via the root-sum-of-square demodulation, these SNR values are quantitatively approximate. Reconstructed SNR values were taken of a 3D volume just encompassing the prostate, in this

case approximately 65 $cm^3$ and comprised of more than 20,000 pixels. Second, using the coil calibration data and assuming the acceleration factors of the DCE-MRI sequence in Table 1, images were formed of the g-factor, a mathematical measure of the ability of a receiver coil array to retain SNR in accelerated MR acquisition (11). These comparisons, shown in Figure 2, indicated that the SNR (A) and g-factor statistics (B) of reconstructions (ii) and (iii) were essentially indistinguishable, and both were different from results for reconstruction (i). Consequently, results for the 12-coil reconstruction were generated in the patient study by selecting data only from those 12 elements from the 32-active-coil acquisition and reconstructing that data. Comparisons were then made with the reconstruction using the full 32-coil data set.

*Radiological Evaluation*

For each of the 50 patient studies the 32-coil DCE-MRI sequence was reconstructed, and 2× magnified images were formed with zero padding which encompassed the prostate. An observer not performing the radiological evaluation selected an axial partition midway through the S/I extent of the prostate at the time frame closest to 50 sec post injection. This typically corresponded to a time 10 to 20 sec after peak contrast enhancement of any rapidly enhancing lesions in the prostate. The magnified 32-coil and 12-coil images from this partition and time frame were then placed side-by-side randomly and in blinded fashion for each study. This set of 50 composite images was then provided to each reviewer.

The two radiologist reviewers (ATF, five years experience in prostate MRI; AK, 20 years experience) then independently graded each image pair using a five-point scale (-2 = left (L) image significantly better than right (R) image; -1 = L slightly better than R; 0 = L and R images

equivalent; +1 = R slightly better than L; +2 = R significantly better than L). This was done for each of the four criteria of perceived SNR, spatial resolution, artifact, and overall preference.

In addition, images of absolute SNR were made for the 32-coil and 12-coil reconstructions for each of the studies using the coil calibration images as described previously for the volunteer study. For this analysis images from the five of the 50 patients who were imaged post-prostatectomy were excluded. For each study the 3D rectangular volume was identified on the reconstructed images which just encompassed the prostate, histograms of the SNR values were generated for all voxels within the volume for the two reconstructions, and the ratio of median values of the 32-coil vs. 12-coil histograms was taken as a measure of SNR improvement for that study. These volumes ranged from 28 to 265 $cm^3$ with a median of 101 $cm^3$, typically including several tens of thousands of pixels. This process was repeated for the g-factor for the acceleration used in the DCE-MRI run, and the ratio of median g-factor values determined.

*Statistical Significance*

For the radiological evaluation after accounting for the blinded presentation, significant (defined as $p<0.05$) difference from the null hypothesis of equivalent performance was assessed with the Wilcoxon signed rank test.

RESULTS

Figure 2B shows the cumulative histograms of the g-factor values for the 32-coil and 12-coil reconstructions. The solid green, blue, and red lines are for the unenhanced test scans of the

volunteer. The green shaded region shows the cumulative g-factor histogram for the 32-coil reconstruction based upon all 50 patient studies. The dashed green line is the median value; the dark green zone encompasses the central 25%, and the light green zone the central 75% at that cumulative percentage. Similarly, the blue shaded region shows analogous results for the 12-coil reconstruction. The more rapid approach to 100% of the green 32-coil reconstruction indicates the overall smaller g-factor values and better retention of SNR vs. the two 12-coil reconstructions (blue curves and blue regions and red curve). This distinction between curves is maintained across all 50 patient studies in that the shaded green and blue regions are well separated. The close match of the blue regions and red curve indicates the equivalence in performance of reconstruction (ii) and (iii).

Figure 3 shows results from the qualitative evaluation of the two radiologists. 32-coil reconstruction (positive scores) was evaluated as significantly superior ($p<.001$) to 12-coil reconstruction using the criteria of SNR (A) and overall preference (D) by both reviewers individually and in aggregate. 32-coil and 12-coil reconstructions were evaluated as equivalent for the criteria of spatial resolution (B) and level of artifact (C) by both reviewers individually and in aggregate. For perceived SNR the two reviewers' scores matched in 38/50 cases and were within one value on the five-point -2 to +2 scale in all 50/50. For artifact these corresponding results were 34/50 and 50/50; for sharpness 27/50 and 46/50; for overall preference 22/50 and 47/50.

Figure 4 shows the percent improvement in SNR values provided by the 32-coil vs. 12-coil reconstruction plotted vs. the BMI of the patient. The red circles show the case with no

acceleration, as determined from the images of SNR using the coil calibration data. The median increase (18%) over the 45 studies is noted with the red hashmark on the ordinate axis, and the trend line, determined by least squares regression, shown in red. The triangles show the case when acceleration is additionally used at the acceleration factors employed in this study with analogous median (32%) and trend lines shown in black.

Figure 5-7 show sample results from three patient studies in which the 32-coil and 12-coil reconstructions are compared.

## DISCUSSION

For the same level of acceleration, the acquisition and reconstruction of data from 32 receiver coils encompassing the pelvis provides superior measured and perceived SNR in dynamic-contrast-enhanced prostate MRI vs. use of the vendor-recommended 12 receiver coils. Although the placement of the 12 receiver elements used encompassed the full lateral and superior/inferior extent of the prostate, the incorporation of data from additional coils can provide improved performance without generation of artifact related to the increase in number of elements.

There are possible disadvantages in the use of additional receiver coils in image reconstruction. When done on the vendor system, the reconstruction time for a 32-coil DCE-MRI run is 50 sec vs. 15 sec on our custom hardware. Lacking high speed computational hardware, another option is to group coil elements together before digitization and reduce the

overall number of data channels (15). As commercial systems continue to improve in the future, reconstruction times are expected to decrease and making this less of an issue.

Another possible disadvantage in the use of incremental coils located somewhat distantly from the FOV of interest is that motion of distant objects might alias into the reconstructed FOV owing to the high sensitivity of the incremental coils to the moving object. The evaluation performed in this work indicated that this was not a significant problem. If artifact were present and could be associated with some specific distant body region, then conceivably the reconstruction could be repeated with data from the coils nearby to that region excluded.

In this work data from each 32-coil DCE-MRI acquisition were reconstructed two ways, the first using all 32 coils and the second using only 12 coils, and the results compared. This study design eliminated the additional uncertainty and expense associated with a study in which each subject would have been imaged twice with contrast material, once with each coil set. We validated this approach by comparing 12-coil reconstruction from 32- and 12-coil acquisitions and showed negligible difference in SNR and g-factor.

This study evaluated two vendor-provided configurations of the coil arrays available with the MRI system. It is possible that other configurations might provide improved performance. Specifically, acceleration applied along a particular direction benefits from coil elements which tend to face each other along that direction. Electrically combining the two most lateral elements of the GEM array into one virtual coil, as done by the vendor, might not be optimal for this array for L/R acceleration. Also, other styles of receiver coil arrays may provide improved

performance, such as arrays placed in better proximity or wrapped around the pelvis. Incorporation of an endorectal coil can be expected to provide some improvement in SNR near that coil. In this work although an endorectal coil was placed in some subjects as seen in Figure 7, it was active only for sequences other than DCE-MRI.

The 32-coil array provided both improvement in SNR and improvement in g-factor statistics vs. the 12-coil array as seen from Figure 4. Both are important for providing improvement in acquisitions such as DCE-MRI in which acceleration is used. It remains to be seen if the improvement solely due to SNR of 32- vs. 12-coil acquisition would benefit non-accelerated sequences. It is interesting that the level of improvement of SNR (red circles of Fig. 4) appeared to correlate positively with BMI.

In addition to the above-described extended reconstruction time and possible motion artifact from distant objects, another limitation of this work is that further study is necessary to determine whether prostate lesion detection and characterization are improved with 32-coil DCE-MRI.

In summary, for the same level of acceleration, the acquisition and reconstruction of data from 32 receiver coils encompassing the pelvis provides superior measured and perceived SNR in dynamic-contrast-enhanced prostate MRI vs. use of 12 receiver coils.

References

1. Delongchamps NB, Rouanne M, Flam T, et al. Multiparametric magnetic resonance imaging for the detection and localization of prostate cancer: combination of T2-weighted, dynamic contrast-enhanced and diffusion-weighted imaging. BJU International. 2010;107:1411-8.

2. Dickinson L, Ahmed HU, Allen C, et al. Magnetic resonance imaging for the detection, localization, and characterization of prostate cancer: recommendations from a European consensus meeting. Eur Urology. 2011;59:477-94.

3. Barentz JO, Richenberg J, Clements R, et al. ESUR prostate MR guidelines 2012. Eur Radiol. 2012;22:746-57.

4. Franiel T, Hamm B, Hricak H. Dynamic contrast-enhanced magnetic resonance iamging and pharmacokinetic models in prostate cancer. Eur Radiol. 2011;21:616-26.

5. Verma S, Turkbey B, Muradyan N, et al. Overview of dynamic contrast-enhanced MRI in prostate cancer diagnosis and management. AJR. 2012;198:1277-88.

6. Rosenkrantz AB, Geppert C, Grimm R, et al. Dynamic contrast-enhanced MRI of the prostate with high spatiotemporal resolution using compressed sensing, parallel imaging, and continuous golden-angle radial sampling: preliminary experience. J Magn Reson Imag. 2015;41:1365-73.

7. Zhu Y, Hardy CJ, Sodickson DK, et al. Highly parallel volumetric imaging with a 32-element RF coil array. Magn Reson in Med. 2004;52:869-77.

8. Gizewski ER, Maderwald S, Wanke I, Goehde S, Forsting M, Ladd ME. Comparison of volume, four- and eight-channel head coils using standard and parallel imaging. Eur Radiol. 2005;15:1555-62.

9. Parikh P, Sandhu G, Blackham K, et al. Evaluation of image quality of a 32-channel versus a 12-channel head coil at 1.5T for MR imaging of the brain. Am J Neuroradiol. 2011;32:365-73.

10. Haider CR, Hu HH, Campeau NG, Huston III J, Riederer SJ. 3D high temporal and spatial resolution contrast-enhanced MR angiography of the whole brain. Magn Reson Med. 2008;60:749-60.

11. Pruessmann KP, Weiger M, Scheidegger MB, Boesiger P. SENSE: sensitivity encoding for fast MRI. Magn Reson Med. 1999;42:952-62.

12. Borisch EA, Trzasko JD, Froemming AT, et al. Faster-than-acquisition 4D sparse reconstruction for Cartesian 2D SENSE-type acquisition. 23rd Annual Mtg, ISMRM. Toronto2015; p. 1580.

13. Kellman P, McVeigh ER. Image reconstruction in SNR units: a general method for SNR measurement. Magn Reson Med. 2005;54:1439-47.

14. Kellman P, McVeigh ER. Erratum to Kellman P, McVeigh ER. Image reconstruction in SNR units: a general method for SNR measurement. Magn Reson Med. 2005;54:1439-1447 Magn Reson Med. 2007;58:211-2.

15. Buehrer M, Pruessmann KP, Boesiger P, Kozerke S. Array compression for MRI with large coil arrays. Magn Reson Med. 2007;57:1131-9.

Table 1. Parameters for 3D RF-spoiled gradient echo prostate DCE-MRI sequence. Acquisition of coil calibration images used the same sequence applied once with phase resolution reduced from 384 to 192.

| Parameter | Value |
|---|---|
| Repetition time (TR) | 5.3 msec |
| Echo time (TE) | 2.2 msec |
| *Field of View | $220 \times 440 \times 114$ mm$^3$ |
| *Sampling Resolution | $256 \times 384 \times 38$ |
| *Spatial Resolution | $0.86 \times 1.15 \times 3.0$ mm$^3$ |
| Acceleration | 2.49 ($R_Y$) × 1.12 ($R_Z$) = 2.78 |
| Frame Time | 6.6 sec |
| Temporal Footprint | ≈ 19 sec |
| Number of Frames | 33 |
| Scan Time | ≈ 3.5 min |

*These parameters are all expressed as (frequency × phase × slice) = (A/P × L/R × S/I).

Figure Legends

Figure 1. Schematics of coil elements and element selection for 12-coil and 32-coil operation. (A) 40-element GEM array contained within the patient table and located posterior to the supine patient. (B) Schematic of 16-element array placed anteriorly to the supine patient. For 12-channel operation the coil elements shown in yellow are selected, eight from the posterior array and four from the anterior array. For 32-channel operation all coils in yellow and additionally those in blue are selected. For the posterior GEM array signals from the lateral-most elements are paired (3 with 33, 4 with 34, etc.) and combined in hardware into one virtual coil per pair. For 32-channel operation all 16 elements of the anterior array are used.

Figure 2. (A) Box and whisker plots of the reconstructed SNR values from the non-contrast-enhanced test case evaluating reconstructions (i) 32-coil acquisition with 32 coil reconstruction, (ii) 32-coil acquisition with 12-coil reconstruction, and (iii) 12-coil acquisition with 12-coil reconstruction. Each figure shows the median, ±25% values (box boundaries), and ±45% boundaries (whiskers). Median values are 28.7, 23.9, and 23.5 (a.u.). (B) Plot of the cumulative g-factor statistics for the 32-channel acquisition with 32-coil (green lines and curves) and 12-coil (blue lines and curves) reconstructions and for the 12-channel acquisition with 12-coil reconstruction (solid red line). The three solid curves are for the non-contrast-enhanced test scans. The shaded green and blue zones show the ranges of g-factor values measured across the 32-coil and 12-coil reconstructions for all 50 patient studies, respectively. The dotted green and blue lines correspond to the median values, the dark shaded zones to ±12.5% about the median and the light shaded zones to ±37.5% about the median. For all plots the statistics are measured over the 3D volume encompassing the prostate.

Figure 3. Histograms showing the results of the radiological review for perceived SNR (A), level of artifact (B), sharpness (C), and overall preference (D). For SNR (A) and overall preference (D) the preference for the 32-coil reconstruction (positive scores) was significant ($p<.001$) for both reviewers individually and in aggregate. For artifact (B) and sharpness (C) there was no significant preference.

Figure 4. Plot of the ratio of median reconstructed SNR values without (red circles) and with (black triangles) the additional effect of g-factor improvements for the 32-coil and 12-coil reconstructions plotted vs. BMI of the patient. In each case values were computed from a volume encompassing the prostate. The median increase for each is shown in the corresponding colored hashmark on the ordinate, and trend lines of each with BMI, as determined from least square regression, are also noted.

Figure 5. Comparison of 12-coil (left) and 32-coil (right) reconstructions of prostate DCE-MRI in a patient with BMI 26.6. Prostate is identified within the white ellipse. Radiologists #1 and #2 both assigned scores of (+2, 0, 0, +2) for (perceived SNR, artifact level, sharpness, overall preference) where positive scores reflect preference for the 32-coil result.

Figure 6. Comparison of 12-coil (left) and 32-coil (right) reconstructions of prostate DCE-MRI in a patient with BMI 30.4. Radiologists #1 and #2 assigned scores of (+1, 0, 0, +1) and (+1, 0, 0, +2).

Figure 7. Comparison of 12-coil (left) and 32-coil (right) reconstructions of prostate DCE-MRI in a patient with BMI 33.4 and with implanted seeds for brachytherapy (black dropouts, e.g. short white arrows). In this exam an endorectal coil used for sequences other than DCE-MRI was applied within a gel-filled insert (long white arrow) but not active for the DCE-MRI sequence. Radiologists #1 and #2 assigned scores of (+1, 0, 0, +1) and (0, 0, 0, 0).

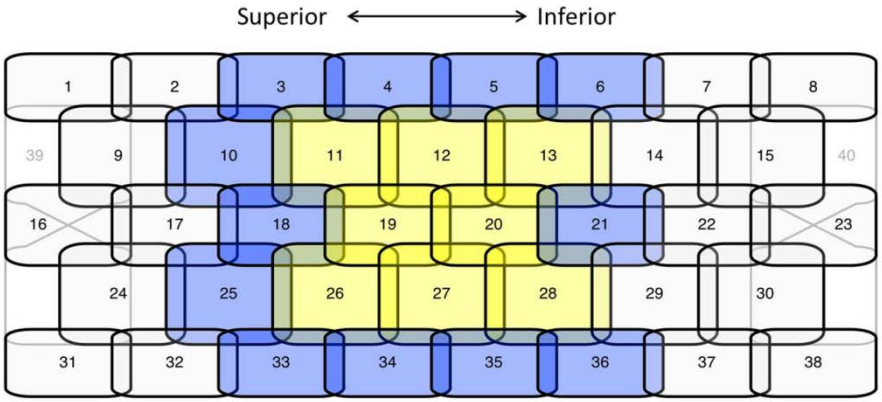


Figure 1. Schematics of coil elements and element selection for 12-coil and 32-coil operation. (A) 40-element GEM array contained within the patient table and located posterior to the supine patient. For 12-channel operation the coil elements shown in yellow are selected, eight from the posterior array and four from the anterior array. For 32-channel operation all coils in yellow and additionally those in blue are selected. For the posterior GEM array signals from the lateral-most elements are paired (3 with 33, 4 with 34, etc.) and combined in hardware into one virtual coil per pair. For 32-channel operation all 16 elements of the anterior array are used.
246x116mm (150 x 150 DPI)

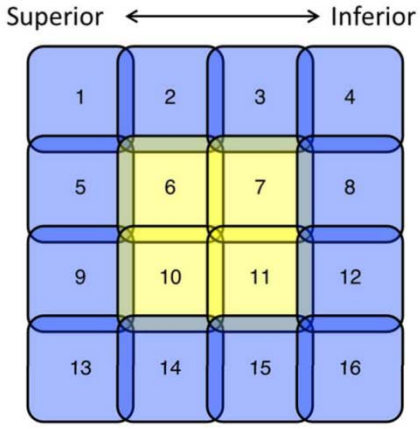


Figure 1. Schematics of coil elements and element selection for 12-coil and 32-coil operation.(B) Schematic of 16-element array placed anteriorly to the supine patient. For 12-channel operation the coil elements shown in yellow are selected, eight from the posterior array and four from the anterior array. For 32-channel operation all coils in yellow and additionally those in blue are selected. For the posterior GEM array signals from the lateral-most elements are paired (3 with 33, 4 with 34, etc.) and combined in hardware into one virtual coil per pair. For 32-channel operation all 16 elements of the anterior array are used.
228x109mm (150 x 150 DPI)

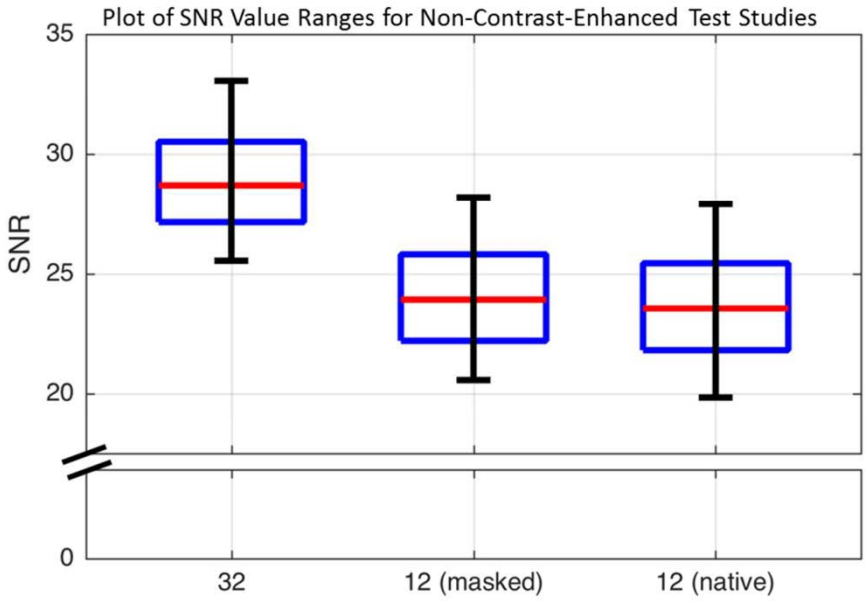


Figure 2. (A) Box and whisker plots of the reconstructed SNR values from the non-contrast-enhanced test case evaluating reconstructions (i) 32-coil acquisition with 32 coil reconstruction, (ii) 32-coil acquisition with 12-coil reconstruction, and (iii) 12-coil acquisition with 12-coil reconstruction. Each figure shows the median, ±25% values (box boundaries), and ±45% boundaries (whiskers). Median values are 28.7, 23.9, and 23.5 (a.u.).
182x117mm (150 x 150 DPI)

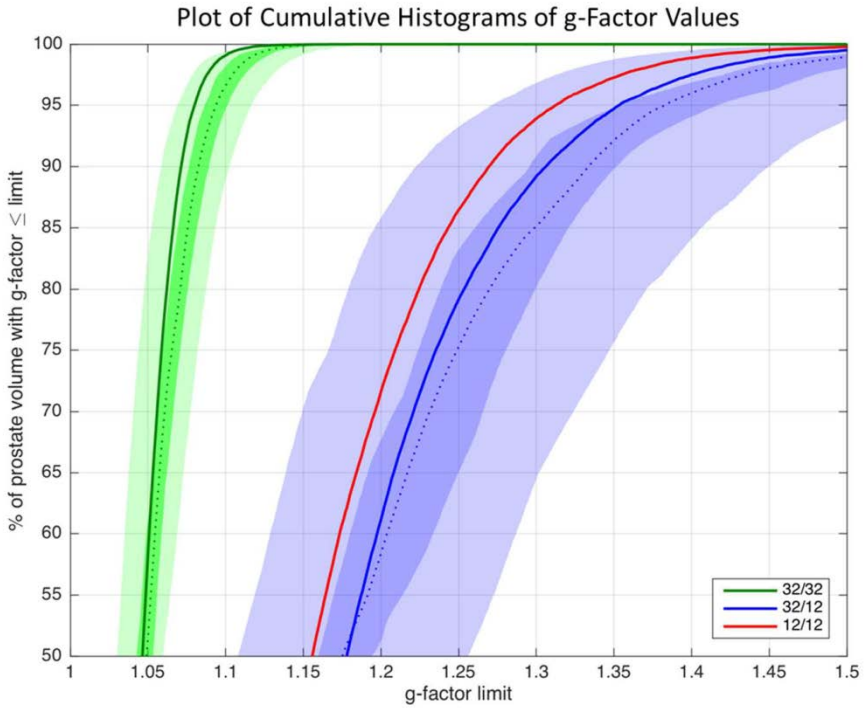


Figure 2. (B) Plot of the cumulative g-factor statistics for the 32-channel acquisition with 32-coil (green lines and curves) and 12-coil (blue lines and curves) reconstructions and for the 12-channel acquisition with 12-coil reconstruction (solid red line). The three solid curves are for the non-contrast-enhanced test scans. The shaded green and blue zones show the ranges of g-factor values measured across the 32-coil and 12-coil reconstructions for all 50 patient studies, respectively. The dotted green and blue lines correspond to the median values, the dark shaded zones to ±12.5% about the median and the light shaded zones to ±37.5% about the median. For all plots the statistics are measured over the 3D volume encompassing the prostate.
197x148mm (150 x 150 DPI)

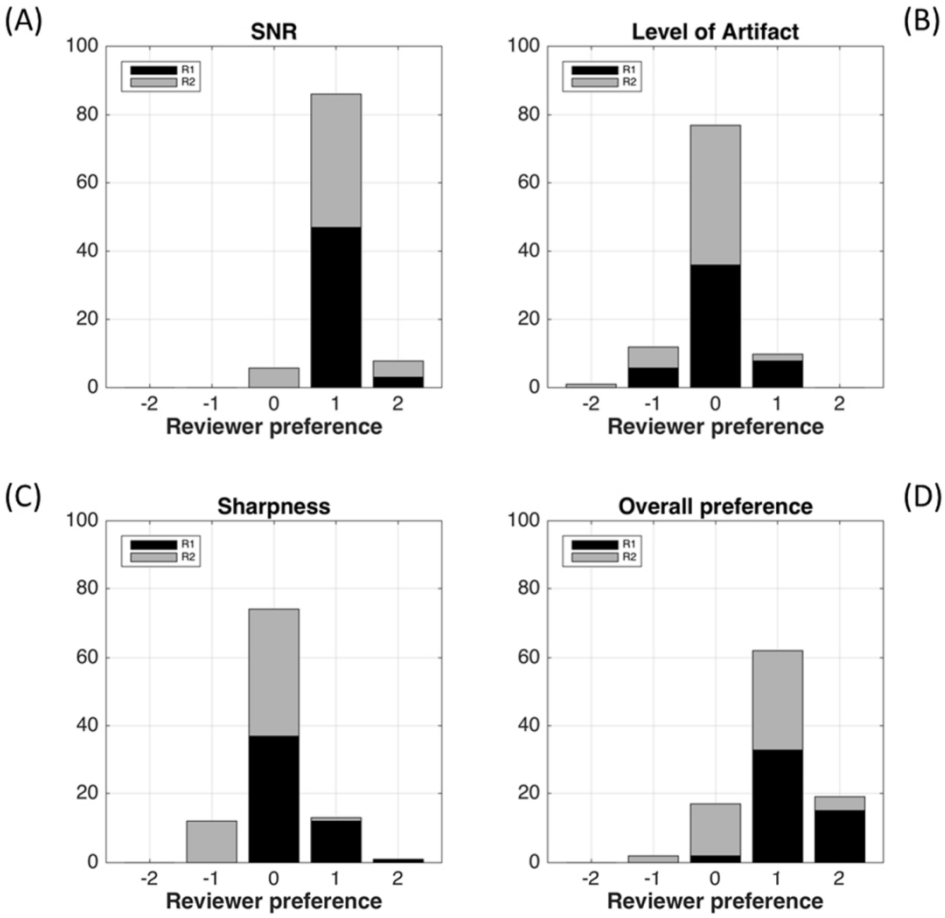


Figure 3. Histograms showing the results of the radiological review for perceived SNR (A), level of artifact (B), sharpness (C), and overall preference (D). For SNR (A) and overall preference (D) the preference for the 32-coil reconstruction (positive scores) was significant ($p<.001$) for both reviewers individually and in aggregate. For artifact (B) and sharpness (C) there was no significant preference.
167x167mm (150 x 150 DPI)

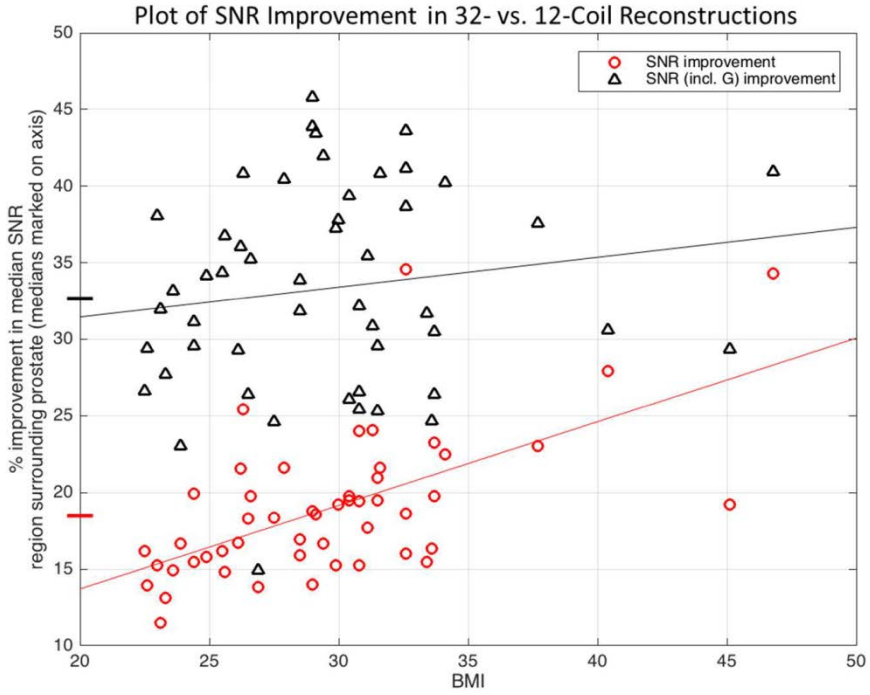


Figure 4. Plot of the ratio of median reconstructed SNR values without (red circles) and with (black triangles) the additional effect of g-factor improvements for the 32-coil and 12-coil reconstructions plotted vs. BMI of the patient. In each case values were computed from a volume encompassing the prostate. The median increase for each is shown in the corresponding colored hashmark on the ordinate, and trend lines of each with BMI, as determined from least square regression, are also noted.
203x152mm (150 x 150 DPI)

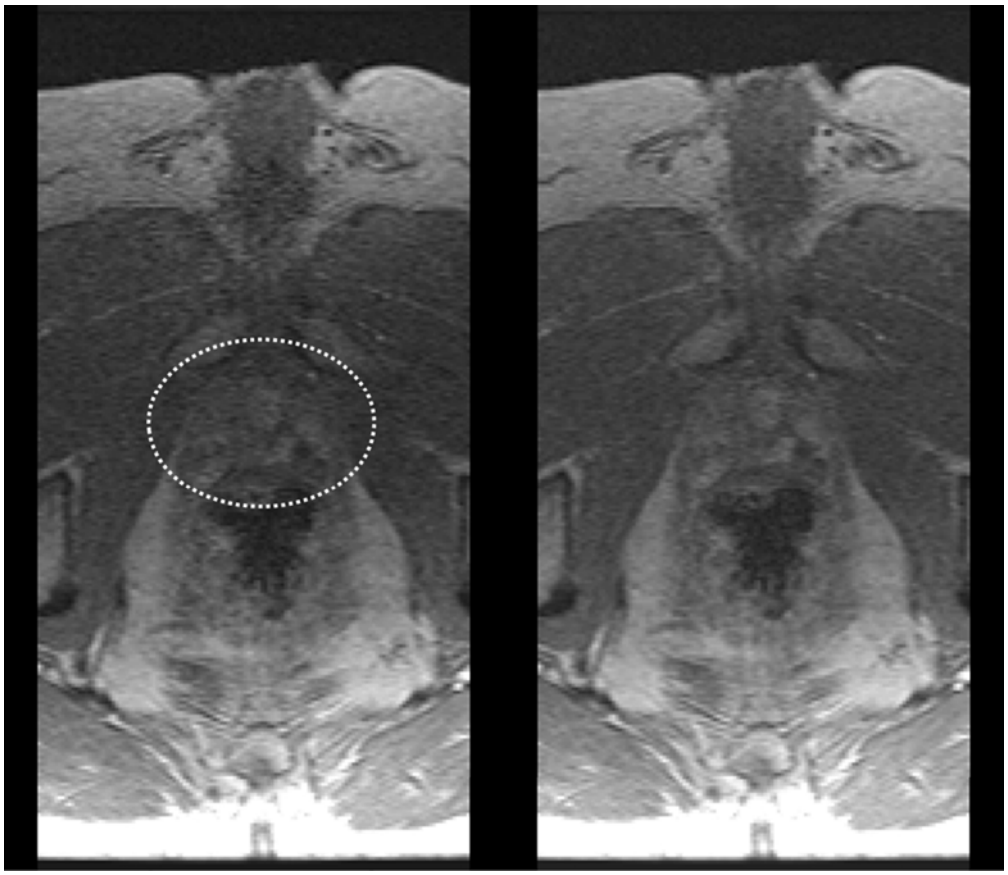

Figure 5. Comparison of 12-coil (left) and 32-coil (right) reconstructions of prostate DCE-MRI in a patient with BMI 26.6. Prostate is identified within the white ellipse. Radiologists #1 and #2 both assigned scores of (+2, 0, 0, +2) for (perceived SNR, artifact level, sharpness, overall preference) where positive scores reflect preference for the 32-coil result.
177x153mm (150 x 150 DPI)

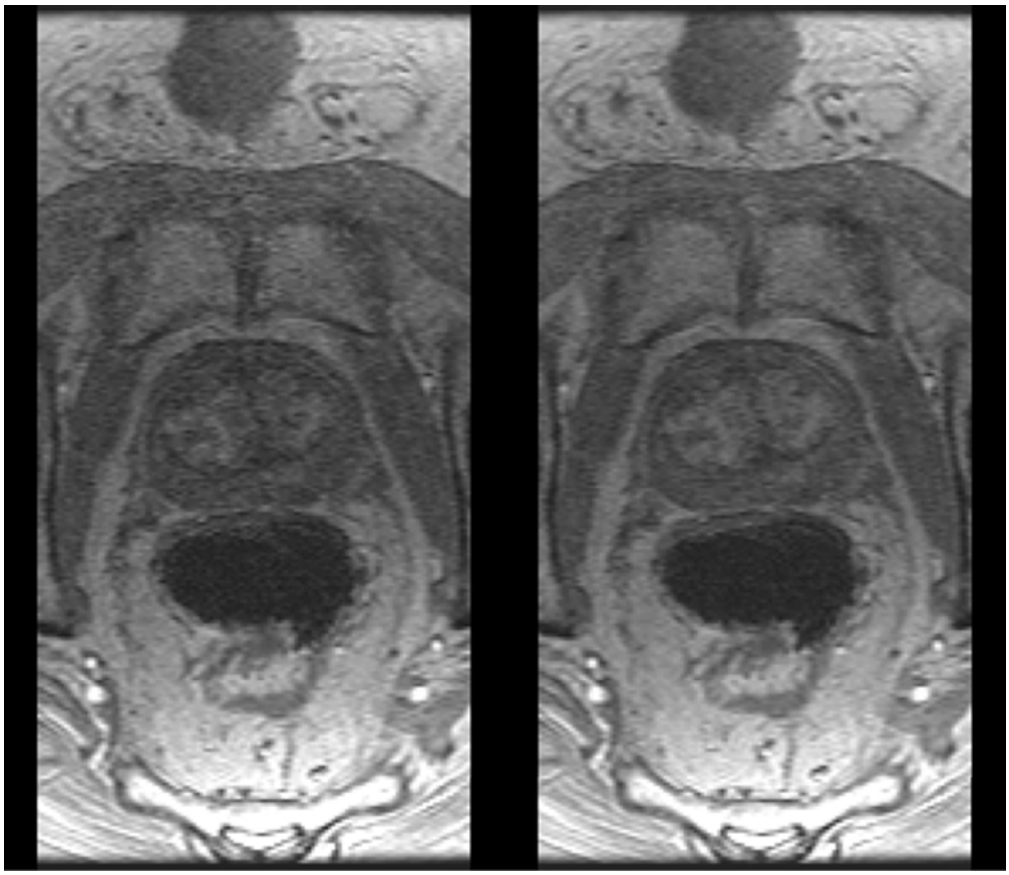

Figure 6. Comparison of 12-coil (left) and 32-coil (right) reconstructions of prostate DCE-MRI in a patient with BMI 30.4. Radiologists #1 and #2 assigned scores of (+1, 0, 0, +1) and (+1, 0, 0, +2).
177x153mm (85 x 85 DPI)

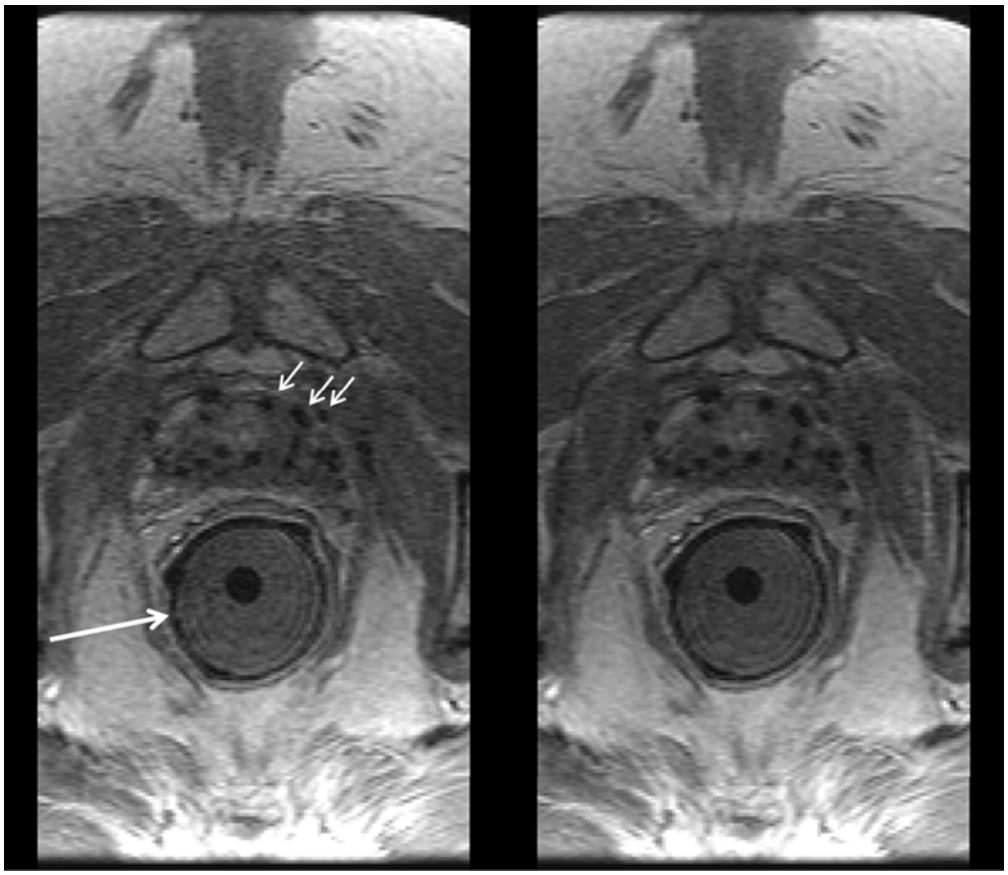

Figure 7. Comparison of 12-coil (left) and 32-coil (right) reconstructions of prostate DCE-MRI in a patient with BMI 33.4 and with implanted seeds for brachytherapy (black dropouts, e.g. short white arrows). In this exam an endorectal coil used for sequences other than DCE-MRI was applied within a gel-filled insert (long white arrow) but not active for the DCE-MRI sequence. Radiologists #1 and #2 assigned scores of (+1, 0, 0, +1) and (0, 0, 0, 0).
177x153mm (150 x 150 DPI)